Korean Journal of Remote Sensing, Vol.17, No.2, 2001, pp.155~164

Reviews

Digital Elevation Map Generation using SAR Stereo Technique with Radarsat Images over Seoul Area

Min-Ho Ka* and Man-Jo Kim**

Dept. of Electrical and Electronic Eng., Yonsei University*, Agency for Defense Development**

Abstract : In this study, we describe the technique for deriving a digital elevation model (DEM) from a synthetic aperture radar (SAR) stereo image pair and apply it to an image pair over "Kwanak-san" in Seoul, Korea. This paper contains brief discussion of the use of stereo SAR to derive topographic data, description of the overall structure of the stereo SAR processing system, description of the site and SAR data used for the evaluation and the source of validation data, results of the stereo SAR processing, analysis and evaluation of their accuracy against map data, and finally summarizes the main highlights of the method used, comments and recommendations on its future implementation.

Key Words : Digital Elevation Map, SAR, Stereo, Radarsat

1. Introduction

1) Stereo SAR

SAR is well known as a provider of remote sensing data in all-weather conditions and has been routinely used in the tropics for over 30 years, primarily to provide geological information to the commercial oil and gas exploration industry (Graham, 1980). To identify or derive topographic data is also problematic over those areas and reliance has generally been placed on the identification of maps, where possible, albeit of variable quality and age. Aerial photography is generally poor over the region due to cloud but also because any blanket coverage of rainforest will mask the topography to some extent. SAR, on the other hand, highlights the topography and therefore should be a good source of such data. Little stereo SAR data has been available from aerial and spaceborne sensors until very recently. The main reason for this is that most antennas have had fixed elevation angles (the angle from Nadir) and therefore the only source of stereo has been from opposite side or overlapping pairs (Leberl, 1980), which are not the most easy (in the first case) or the most accurate (in the latter) cases to use. Even ERS-1 and 2 have fixed elevation angles, although the ERS-1 satellite was physically steered to increase the elevation angle from approximately 23° to 35° for one month during a

Received 20 November 2000 ; Accepted 20 April 2001.

"Roll-Tilt" Mode. In 1995, the Canadian Radarsat satellite was launched as a commercial provider of stereo SAR data worldwide (RSI, 1995). Radarsat has a steerable antenna and is therefore able to view from elevation angles between 20° and 50°. The configuration of the satellite and its ground segment mean that good quality stereo data could be available. The imminent launch of the European ENVISAT satellite which has a similar capability (ESA, 1997) and after this, Radarsat-2 means that such data will be available for years to come.

2) Principle

The Stereo SAR technique is very well understood, obviously deriving from the corresponding optical technique but with some refinements to use radargrammetric, as opposed to photogrammetric, principles. Radar is very different to optical in the way that data is organized and most successful methods use a radar methodology. However, good approximations can be made by approximating a photogrammetric model, especially over small areas, which are computationally more efficient. The basis of any stereo process is that, by looking at the same point from two different positions in space, we can calculate the full three-dimensional position of that point. This is illustrated in Fig. 1 below.

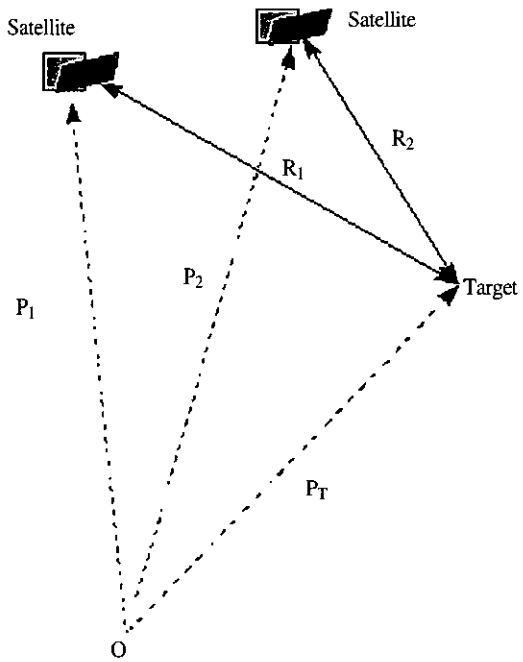

Fig. 1. The Radar Stereo Principle.

In Fig. 1, the target is imaged from a sensor at two different positions in orbit, given by the position vectors P_1 and P_2 related to the origin of the Earth at O. In radar, the important geometrical parameters are the value of the Doppler Centroid, which gives the look angle (angle from nadir), and the slant range, which is the distance from the sensor to the target, given here as values R_1 and R_2 in the figure. From these parameters, and an orbit model, it is possible to derive the three-dimensional position vector of the target point, P_T. Using standard geodetic equations, the three-dimensional position vector P_T can be transformed into map coordinates (e.g. Northings and Eastings) and a height above a reference ellipsoid or geoid. When arranged into a regular map coordinate grid, the heights are referred to as a DEM.

2. Geometric Accuracy

Stereo SAR pairs can, by definition, only be approached by two schemes, same side and opposite side, due to the side-looking nature of the instrument. Opposite side views give by far the greater accuracy, having the greatest disparity between the two views. However, the views look completely different and can only be matched using a mostly manual process which is time

consuming and expensive. Same side views are much easier to match automatically, looking very much the same, and so are much easier and quicker to process, although at the cost of accuracy. The geometric accuracy of any information derived from any source depends on two factors:

- Localization: This relates to the positional accuracy of the data (i.e. how accurately it can be located on the Earths surface) and is generally dependent on the accuracy of a number of parameters such as image timing, orbit accuracy, image processing, and etc.
- Spatial Resolution: This relates to our ability to distinguish two separate targets within an image. The spatial resolution is defined as the minimum distance two targets have to be apart in order for us to be able to say, with confidence, that they are, indeed, two targets.

For a stereo-derived product, both factors influence the final accuracy. In terms of localization, relating to the positional accuracy of heights or pixels, the accuracy is variable. For Radarsat data, this information is not readily available but is anticipated to be better than 500 m without ground control (RSI, 1995). Obviously, if ground control points (GCPs) are available, then the localization accuracy can be improved to the order of the spatial resolution which, for Standard Mode data is 30 m. The height accuracy is wholly dependent on the spatial resolution and the difference in look angle between the stereo views. Consider the same-side viewing configuration illustrated in Fig. 2 where we have a target at height h viewed at incidence angles θ_1 and θ_2 respectively.

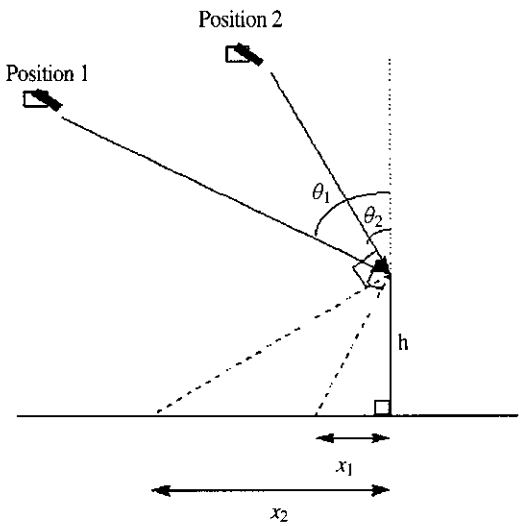

Fig. 2. Same Side Stereo Imaging Geometry.

From simple trigonometry, we can show that the displacement of the target from its true position when viewed from Position 1, caused by the foreshortening effect of the radar, is given by x_1 where:

$$x_1 = h \cot\theta_1.$$

Similarly, the displacement caused by viewing from Position 2 is given by x_2 where

$$x_2 = h \cot\theta_2.$$

If we are to gain stereo information from the two views, the only condition is that the difference in displacement caused by viewing from the two positions is measurable. This means, simply, that:

$$| x_2 - x_1 | \geq \rho$$

where ρ is the spatial resolution of the image.

We can easily invert this equation to find the minimum height difference measurable from stereo SAR for any given spatial resolution and incidence angle. This is:

$$H = \rho / (\cot\theta_2 - \cot\theta_1)$$

where H is the minimum height resolvable.

The value of H is calculated for a number of representative combinations of Radarsat and ERS

Table 1. Minimum Height Resolvable from Various SAR Image Combinations.

Combination	Angular Range (degrees)	H (metres)
ERS PRI Near and Far Range	19-26	35.1
Radarsat S1 and S7	23-47	21.1
Radarsat S2 and S7	27-47	29.1
Radarsat F1 and F5	38-47	25.5

data, assuming same side geometry. The value of H shown in Table 1 is the relative height of a stereo SAR-derived DEM.

3. Stereo SAR System Description

The overall stereo SAR system is illustrated in Fig. 3.

Essentially, the stages in the processing are as follows.

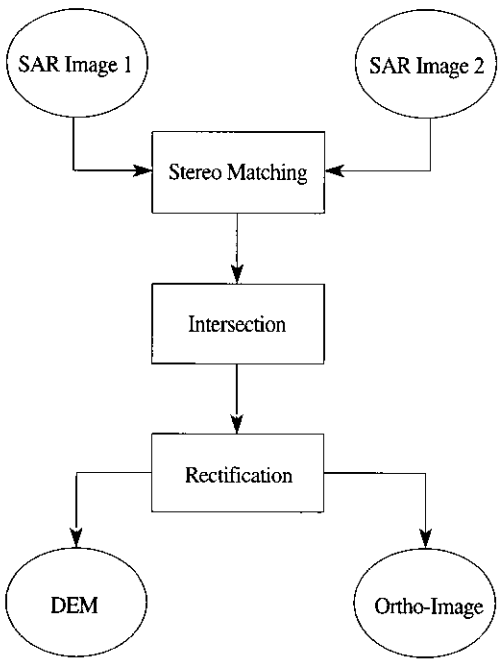

Fig. 3. Overall Stereo SAR System.

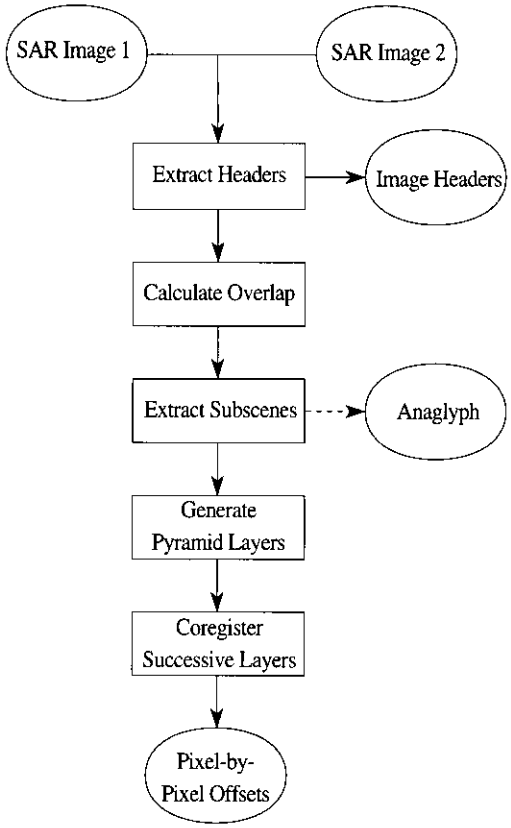

Fig. 4. Stereo Matching Processing Chain.

1) Stereo Matching

This covers all aspects of data input and the matching itself, which involves the systematic identification of the same points in the two different images. For the matching, a coarse to fine pyramidal method is used which essentially begins matching at a low resolution and refines the process as we approach full resolution. The basic stereo matching processing chain is shown in Fig. 4. Note that there is an option to output a stereo anaglyph automatically from this process.

2) Intersection

Intersection is a well-defined problem and has been approached through photogrammetric

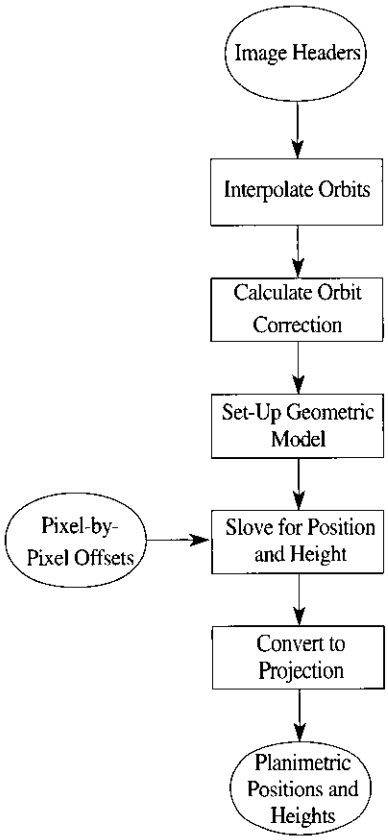

Fig. 5. Intersection Processing Chain.

modeling (Toutin and Carbonneau, 1992) and, more appropriately through radargrammetric modeling (Dowman *et al.*, 1997; Toutin, 1997). Here, the disparity between the two images is converted into a height and grid reference using a specified ellipsoid and datum as reference and, nominally the Universal Transverse Mercator (UTM) projection. The Intersection Processing Chain is shown in Fig. 5. In this part of the algorithm, a correction to the orbit is applied. This is very important if the orbit is poorly specified, as it is for Radarsat data, as it allows the generation of a more reliable and accurate product.

3) Rectification

Here, the irregular grid of positions and heights

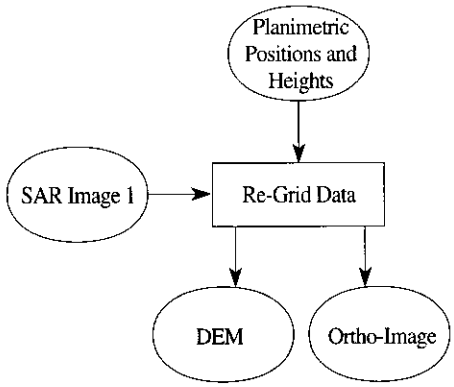

Fig. 6. Rectification Processing Chain.

is placed into a regular map projection grid, essentially rectifying and geocoding the data. The processing chain is illustrated in Fig. 6. Note that a rectified image is also produced in the same coordinate system.

4. Site Description and Input Data

The site chosen for this study is around "Kwanak-san" in Seoul, Korea. The mountain consists of two peaks at heights of around 400m and 600m above the city. The peaks are separated by a distinct valley. The mountain itself is covered in forest, which has created some problems in deriving a DEM through SAR interferometry as the coherence is generally lower than areas

Table 2. Radarsat Data Characteristics.

	Image 1	Image 2
Scene Date	27 December 1996	8 December 1997
Scene Time	09:30:47.556 GMT	09:39:11.807 GMT
Beam Mode	Fine 1	Fine 5
Orbit	5986 - Ascending	10931 - Ascending
Product Type	Path Image	Path Image
Product Size	8037 lines x 7152 pixels	8095 lines x 6117 pixels
Pixel Spacing	6.25m	6.25m
Incidence Angle	38.277 degs	46.357 degs

without forest. Therefore, the site offers a good chance to demonstrate the complementarity of the technique with stereo SAR. For the stereo analysis, two Radarsat Fine Beam Mode images of the site were prepared. Their details are given in Table 2.

Images of the two SAR scenes which include "Kwanak-san" are shown in Fig. 7 and Fig. 8. It is clear that both images do not cover exactly the same area - the Fine 1 image is slightly shifted to the East than the Fine 5 image. However, there is

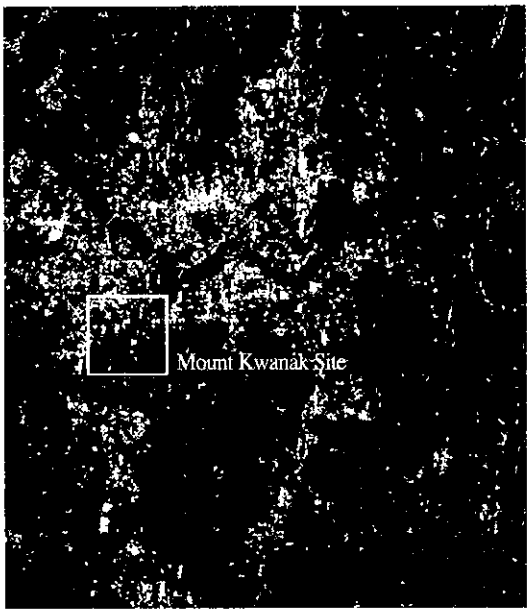

Fig. 7. Radarsat Fine 1 Image of Study Site.

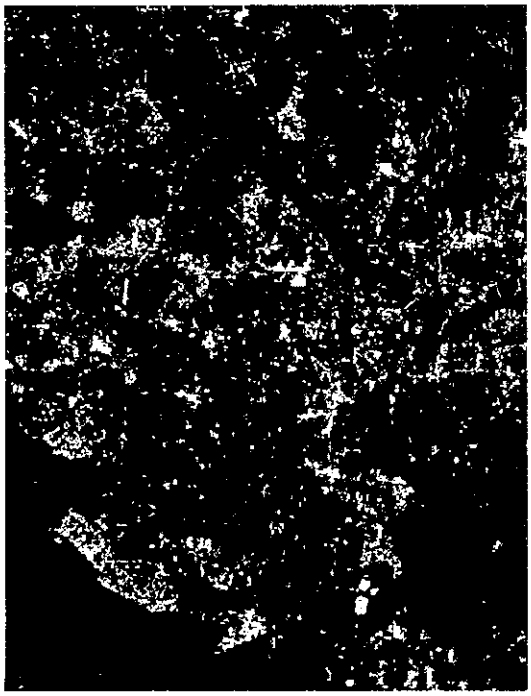

Fig. 8. Radarsat Fine 5 Image of Study Site.

Fig. 9. Radarsat Anaglyph of Study Site (this needs to be viewed through red/green spectacles).

an overlap between the two centered on the city itself, allowing a stereo analysis to be performed. The city stands out clear as the bright area between the mountains. The Han river runs from East to West and is rendered as the thick dark linear feature dividing the image. The area of overlap is illustrated in the anaglyph (Fig. 9) where the Fine 5 image is coloured red and blue and the Fine 1 image green. The anaglyph is best viewed through red/green spectacles which allow the topography to be fully appreciated, contrasting the relatively flat areas of the city with the hills and mountains surrounding it.

For validation of stereo processing, it is important to have an independent source of topographic data. Over this area, we have been provided with a Digital Terrain Elevation Data (DTED) Level 1 3-arc second data generated by the National Imagery and Mapping Agency and distributed by the United States Geological Survey (USGS). The data has been transformed into a UTM projection using ERDAS IMAGINE® and output at 20m grid spacings. Details are given in Table 3.

Table 3. DTED Parameters.

Horizontal and Elevation Accuracy,resp.	50m , +/- 30m
Grid Spacing	20m
Horizontal Datum	WGS 84
Vertical Datum	WGS 84
Projection	UTM Zone 52 North

5. Generation of Topographic Data over Study Site

Images of the "Kwanak-san" site are shown in Fig. 10 below.

As is clear from the figure, Mount Kwanak itself occupies the bottom half of the site. The mountain has two peaks either side of a valley rising to approximately 400 m and 600 m above the level of the urban area in the top half of the image. The mountain is almost wholly covered in forestry. Interestingly, although the images were acquired a year apart, there is very little temporal change between them apart from a small area in the urban area in the upper right portion of the image. This is interesting to note as it will almost

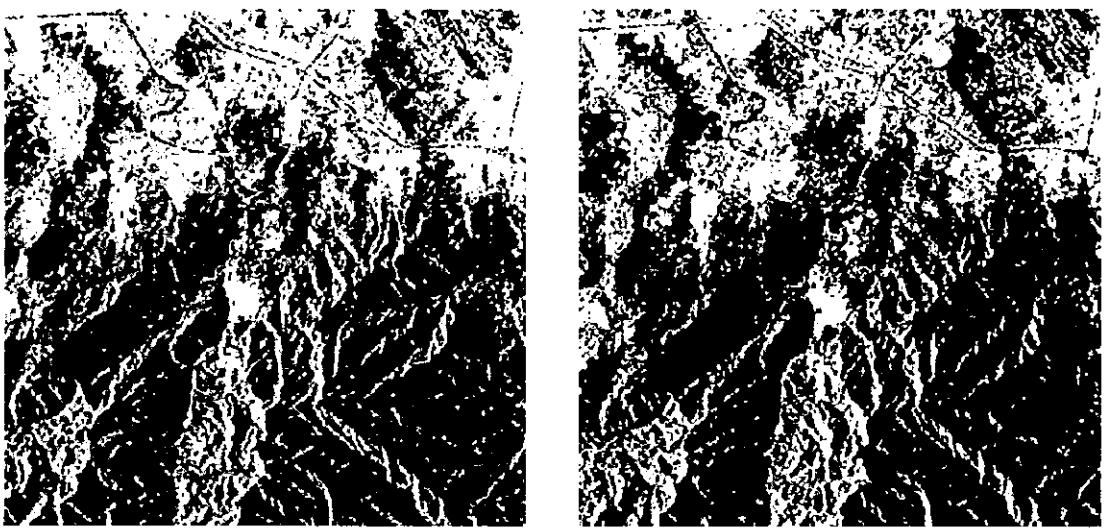

Fig. 10. Fine 1 (left) and Fine 5 (right) Images of Study Site.

certainly create a problem for the stereo matcher. Rendered three-dimensional views of the stereo SAR-derived DEM and the DTED DEM are shown in Fig. 11 and Fig. 12, respectively. Fig. 11 is rectified to UTM Zone 52 North using the Tokyo-B datum as reference. All heights derived by the stereo analysis are referenced to the Bessel ellipsoid. From a qualitative point of view, the results successfully represent the area in question in that the mountainous area is shown as two peaks separated by a valley. Comparisons with the DTED data show that, there is agreement between the ridge and valley structures. Profiles of the topography running North-South and West-East are shown in Fig. 13 and Fig. 14. It is clear from both sets of profiles that there is a small offset between the height values from stereo and DTED values. Since both sets have derived heights referred to different ellipsoids, this is most likely to be the cause of this. Otherwise, agreement between them is excellent on both the shape of the topography and the relative height values between points. The slope down to the city from the mountain shows excellent agreement with the DTED value. The West-East profile is more noisy but, essentially, the positions and values of the peaks seem to agree. The quantitative agreement between the profiles is encouraging as the stereo DEM is derived with no ground control at all.

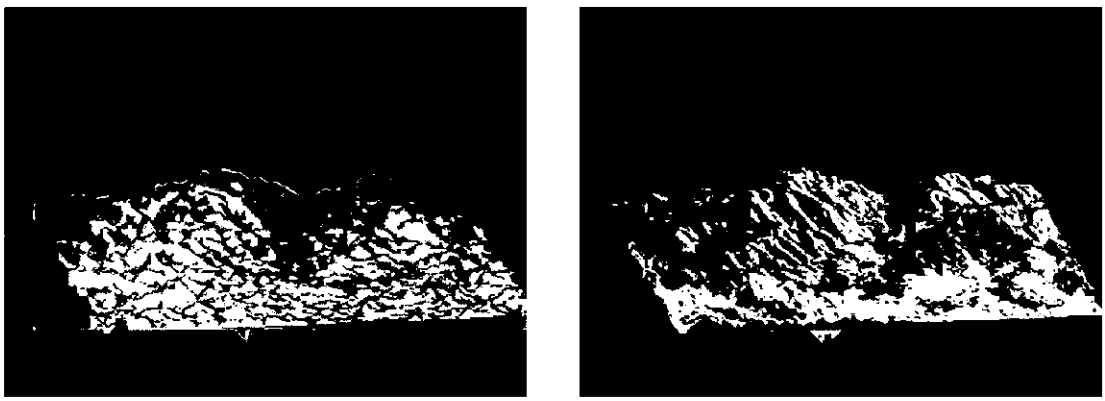

Fig. 11. Stereo SAR-derived DEM (left) and Rendered Image (right) Viewed from North.

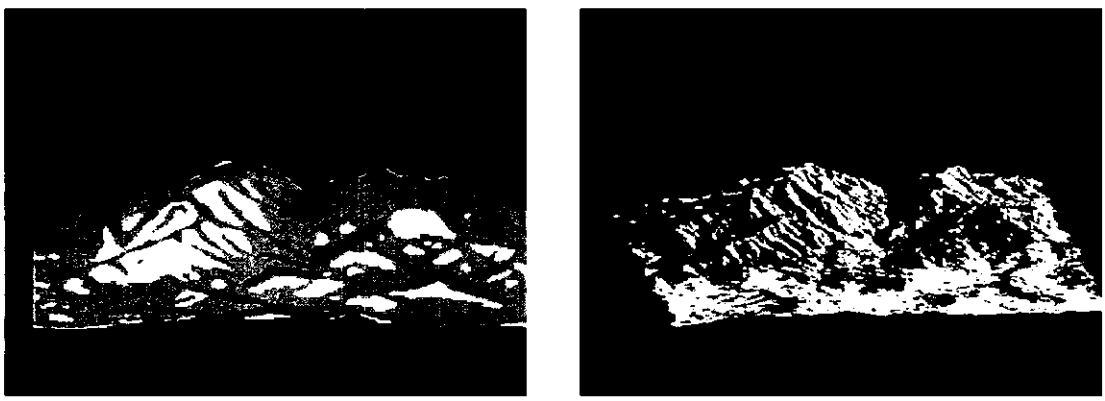

Fig. 12. DTED DEM (left) and Rendered Image (right) Viewed from North.

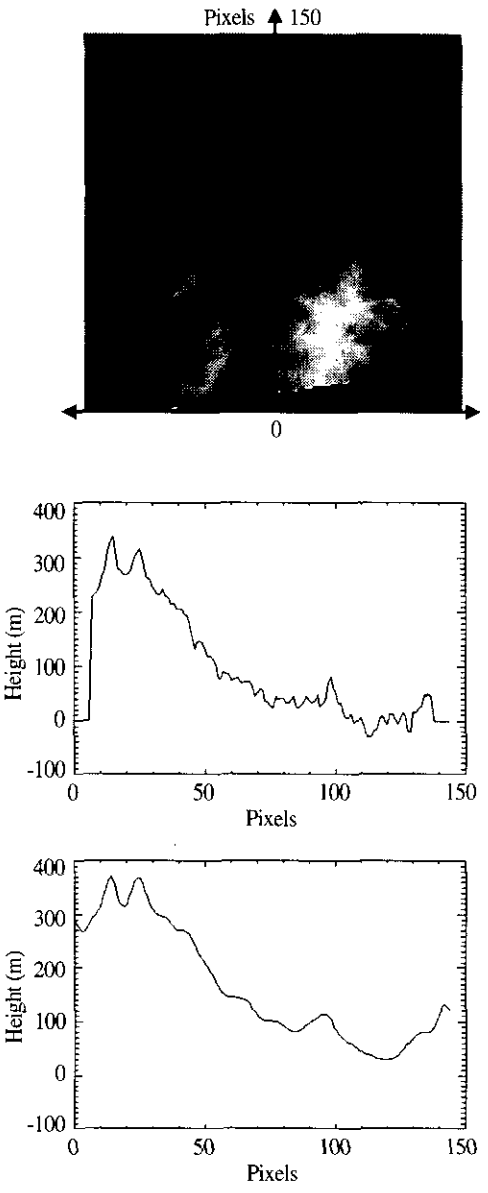

Fig. 13. Profiles taken along Center South-North Direction (illustrated at top) from Stereo-Derived DEM (center) and from DTED (bottom).

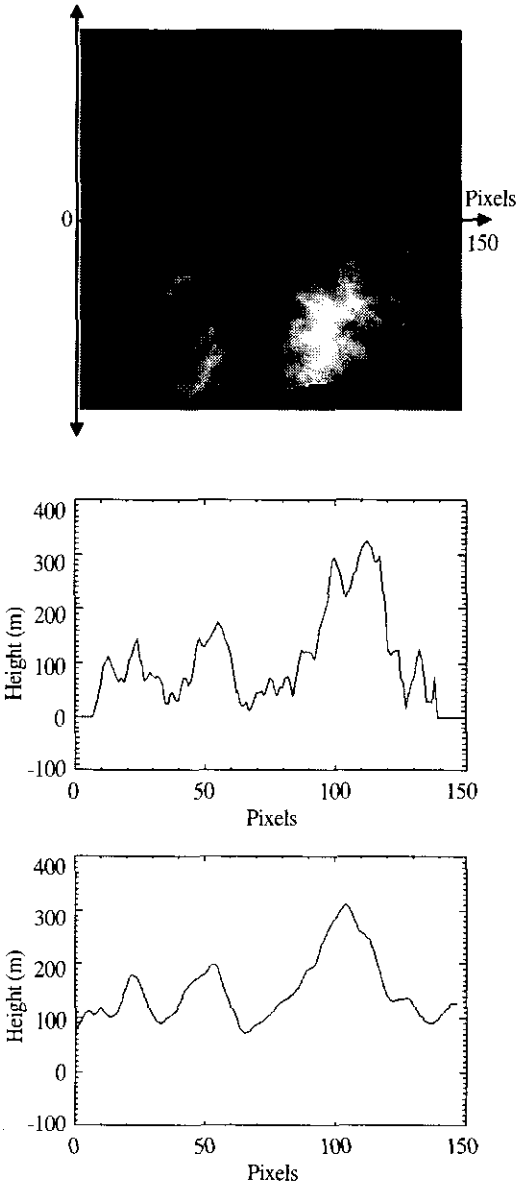

Fig. 14. Profiles taken along Center West-East Direction (illustrated at top) from Stereo-Derived DEM (center) and from DTED (bottom).

The following observations were made during the analysis:

- Results show general visual agreement when profiles are drawn of the topography. This illustrates the generally good result of both the matching and the intersection processes.
- Areas of temporal change between the two dates did produce errors in the DEM.

Probably, the main recommendation is to underline the detrimental effect of layover and

shadow and, through selection of incidence angles and modes, to try to avoid them at all costs.

6. Conclusions

The results described above show conclusively that it is possible to derive topographic data from stereo SAR data. Furthermore, all data products shown were derived with no ground control or manual massaging of the results. Essentially, what is seen here is what is output by the process. This is an important observation, as the cost of generating such information is the most important factor in determining the commercial use of the method. A preliminary quality assessment is described above over a specific area of interest in Seoul, Korea. The results show that stereo SAR technique is useful as they can produce topographic maps at scales between 1:50000 and 1:100000 over such areas. Theoretically, on the basis of spatial resolution alone, it is possible to derive a DEM at scales better than 1:50000, but this does not take into account the excessive noise of single look data which causes a much greater problem if we require a higher resolution product. In this case, further experimentation with speckle filters and matching kernels is required to improve the match without too much blurring of the resolution, preserving point and linear features wherever possible. The main conclusion from this analysis is that accurate stereo-derived information can be derived from SAR data and could be a effective way of deriving such information.

Acknowledgement

This research has been performed jointly by ADD (Agency for Defense Development) and MMS (Matra Marconi Space), UK.

References

Graham, L., 1980, Stereo Radar for Mapping and Interpretation in Radar Geology: An Assessment(Report of the Radar Geology Workshop, Snowmass, Colorado, July 16-20, 1979), *JPL Publication.*

Leberl, F., 1980, Application of Imaging Radar to Mapping in Radar Geology: An Assessment(Report of the Radar Geology Workshop, Snowmass, Colorado, July 16-20, 1979), *JPL Publication.*

RSI, 1995, *RADARSAT Illuminated. Your Guide to Products and Services*, Radarsat International Client Services, Canada.

ESA, 1997, *ENVISAT-1 Mission and System Summary*, European Space Agency.

Toutin, T. and Carbonneau, Y., 1992, MOS and SEASAT Image Geometric Corrections, *IEEE Trans. on Geoscience and Remote Sensing*, 30 (3).

Dowman, I., Twu, Z.-G. and Pu-Huai, C., 1997, DEM Generation from Stereoscopic SAR, *Proceedings of the First Radarsat Applications Symposium*, Canada, April 1997.

Toutin T., 1997, Accuracy assessment of stereo-extracted data from airborne SAR images, *International Journal of Remote Sensing*, 18 (18): 3693 - 3707.